Metabolite Predictions for Para-Substituted Anisoles Based on *Ab Initio* Complete Active Space Self-Consistent Field Calculations

Marcel J. de Groot,[†,‡] Gabriëlle M. Donné-Op den Kelder,[†,‡] Jan N. M. Commandeur,[†] Joop H. van Lenthe,[§] and Nico P. E. Vermeulen*,[†]

Leiden/Amsterdam Center for Drug Research, Divisions of Molecular Toxicology and Medicinal Chemistry, Department of Pharmacochemistry, Vrije Universiteit, De Boelelaan 1083, 1081HV Amsterdam, The Netherlands, and Debye Institute, Theoretical Chemistry Group, Utrecht University, Padualaan 14, 3584CD Utrecht, The Netherlands

Received September 20, 1994[⊗]

The cytochrome P450 mediated oxidative metabolism of a series of para-substituted anisoles has been examined using *ab initio* CASSCF (complete active space self-consistent field) calculations. On the basis of these calculations, oxidative metabolites were rationalized using the concept of hydrogen atom abstraction, spin delocalization, and hydroxyl radical recombination, which is believed to govern part of the oxidation and oxygenation reactions catalyzed by cytochrome P450. Spin distributions and energy differences between substrates, metabolic intermediates, and products were calculated. A comparison of the predictions with recent experimental findings from other laboratories supports the applicability of the currently used computational model for predicting qualitatively the oxidative metabolism by cytochrome P450.

Introduction

Cytochromes P450 (P450)[1] belong to a group of iron heme-containing proteins which catalyze oxygenation, oxidation, and reduction reactions. Oxygenation involves insertion of one oxygen atom from molecular oxygen into substrates, with concomitant reduction of the other oxygen atom to water (*1*). The reducing equivalents are donated by an external donor, such as NADPH cytochrome P450 reductase or NADPH cytochrome b_5 reductase. The incorporation of oxygen into substrates does not proceed spontaneously at appreciable rates as ground state molecular oxygen is in a triplet (diradical) electronic configuration while most organic compounds (and their oxygenated products) are in a paired singlet electronic configuration. During the proposed reaction between triplet dioxygen and a singlet substrate, a short-lived high energy (triplet) transition state is formed in which spin-inversion (to allow spin-pairing) will normally not be established, so no reaction will take place. However, in the case of P450, spin-inversion is facilitated by the iron heme group in the active site of the protein (*2, 3*).

P450 enzymes catalyze the oxidation and oxygenation of a wide variety of compounds. For these reactions, various mechanisms have been proposed in literature, e.g., via initial hydrogen atom abstraction (*2, 4–9*), via one-electron oxidation (*2, 4, 5, 10*), or via direct addition of a ferryl oxygen to a π-bond or lone pair (*11, 12*). Among others, based on large (in some cases >10) observed kinetic isotope effects, alkane hydroxylations are suggested to occur via initial hydrogen atom abstraction (*2*). On the basis of relatively low (<2) inter- and intramolecular kinetic isotope effects, amine dealkylations are thought to occur via a one-electron oxidation mechanism (*1, 10, 13*). The aromatic hydroxylation of monofluoroanilines, however, has been suggested to take place via electrophilic attack of the (heme-FeO)$^{3+}$ species on a specific carbon of the aromatic ring (*12*).

The chemical oxidation of several aromatic substrates has been studied extensively. Anodic acetoxylation of anisole (**1**) (Figure 1), which closely resembles an electrophilic aromatic substitution reaction catalyzed by P450, is reported to produce mainly ortho- and para-acetylated products (*14*). The chemical oxidation of *p*-methylanisole (**2**) (Figure 1), with manganese(III) acetate and a variety of other chemical one-electron oxidants, primarily gives acetylation at the benzylic carbon (*14, 15*), finally yielding *p*-methoxybenzyl acetate (*16*). Shono *et al.* have examined the anodic oxidation of *p*-cyclopropylanisole (**3**) (Figure 1), but no products were reported (*17*). Free radical chlorination of *p*-cyclopropylanisole (**3**) has been reported to give chlorination primarily at the ortho position, but also at the para position, relative to the methoxy moiety (*16*).

Concerning the enzymatic P450 oxidation of aromatic substrates, more data are available. For a series of deuterated toluenes large kinetic isotope effects (KIEs) have been reported (*18, 19*) as well as the relative amounts of metabolic products: benzyl alcohol (65%), *o*-cresol (15%), *m*-cresol (5%), and *p*-cresol (15%) (for toluene-d_0) (*18*). With increasing deuteration of the methyl group, metabolic switching from the formation of benzylic alcohol to cresol was observed. In a recent study, Riley and Hanzlik investigated the metabolism of cyclopropylbenzene and *p*-cyclopropylanisole (**3**) in rat liver microsomes (*20*). The metabolites of cyclopropyl-

* To whom correspondence should be addressed.
[†] Division of Molecular Toxicology, Vrije Universiteit.
[‡] Division of Medicinal Chemistry, Vrije Universiteit.
[§] Utrecht University.
[⊗] Abstract published in *Advance ACS Abstracts,* March 15, 1995.
[1] Abbreviations: au, atomic unit of energy (1 au = 2625.5 kJ/mol); βNF, β-naphthoflavone; CASSCF, complete active space self-consistent field; DMA, distributed multipole analysis; ΔE, energy difference; GAMESS-UK, Generalised Atomic and Molecular Electronic Structure System UK version; $\Delta H^{\ddagger}$, activation energy; ΔH_R, heat of reaction; HOMO, highest occupied molecular orbital; LUMO, lowest unoccupied molecular orbital; MCSCF, multiconfiguration self-consistent field; NAPQI, *N*-acetyl-*p*-benzoquinone imine; P450, cytochrome P450; RHF, restricted Hartree Fock; STO, Slater type orbital; SV, split valence; UHF, unrestricted Hartree Fock.

0893-228x/95/2708-0437$09.00/0

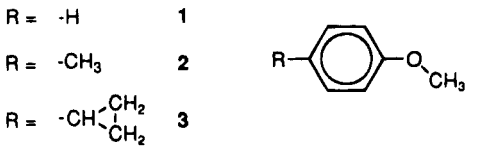

Figure 1. Substrates under investigation: anisole (**1**), *p*-methylanisole (**2**), and *p*-cyclopropylanisole (**3**).

benzene were found to be 1-phenylcyclopropanol, 4-cyclopropylphenol, and 2-cyclopropylphenol, the formation of 1-phenylcyclopropanol being explained by a hydrogen atom abstraction, radical recombination mechanism. The preferred metabolic pathways of *p*-cyclopropylanisole were shown to be O-demethylation (>90%) and benzylic hydroxylation (*20*).

Arylcyclopropanes containing a benzylic hydrogen have been suggested to be suitable probes for differentiating between hydrogen atom abstraction and one-electron oxidation mechanisms (*16, 20*). It is thereby assumed that a one-electron abstraction from the π-system does not lead to deprotonation at the benzylic carbon, but rather to cyclopropyl ring opening (*16*). No ring opened metabolites were found for cyclopropylbenzene and *p*-cyclopropylanisole. The oxygenation mechanism involved in the benzylic hydroxylation reaction was therefore proposed to be consistent with hydrogen atom abstraction and radical recombination (*20*). The O-demethylation of *p*-cyclopropylanisole and the aromatic hydroxylation of cyclopropylbenzene, both leading to the formation of *p*-cyclopropylphenol, were explained by α-hydroxylation and a classical mechanism, respectively (*20*).

The research presented here describes the application of an *ab initio* quantum chemistry based theoretical approach to investigate possible P450 oxidation mechanisms. The hydrogen atom abstraction, spin delocalization, hydroxyl radical recombination mechanism, as proposed by various authors (*2, 7, 8, 21*), is used to estimate the probability of the oxygenated metabolites of various anisoles **1**, **2**, and **3** (Figure 1). The compounds investigated theoretically for this paper were selected on the basis of the literature mentioned above. Based on calculated energy differences between substrates, metabolic intermediates and products, and spin distributions of intermediate radicals, predictions will be done concerning the most probable metabolic pathways/metabolites. The influence of both substituents para to the methoxy group upon the possible metabolic routes is investigated.

Computational Methods

The quantum chemical program package GAMESS-UK (*22, 23*) was used for the *ab initio* calculations. The initial conformation of anisole (**1**) was generated with the modeling package ChemX (*24*). Starting from this initial conformation several other conformations were generated manually. All conformations were optimized at the RHF (restricted Hartree Fock) level with the STO-3G (Slater type orbitals comprized of 3 Gaussians) (*25*) minimal basis set, and the lowest energy conformation was selected. The starting conformations of intermediates and products were constructed from the optimized geometry of the starting compound (**1**). The optimized geometries of anisole (**1**) and its intermediates and products were used as starting conformations for the para-substituted anisoles (**2** and **3**) and their metabolic intermediates and products.

The resulting geometries were further optimized with a minimal (STO-3G) basis set using the CASSCF method (*26–28*) starting from UHF (unrestricted Hartree Fock)-derived natural orbitals (*29, 30*). In the CASSCF treatment (or more generally the MCSCF (multiconfiguration self-consistent field) treatment), both orbitals and configuration coefficients are optimized in a multiconfiguration wavefunction. This is done in order to incorporate electron correlation in the calculations, which is needed, for example, to describe breaking of covalent bonds and formation of radicals (*29*). The calculations were performed within a 4*4 active space (HOMO-1, HOMO (highest occupied molecular orbital), LUMO (lowest unoccupied molecular orbital), LUMO+1) for the closed shell species (starting compounds, neutral intermediates, and products) and a 5*5 active space (HOMO-2, HOMO-1, HOMO, LUMO, LUMO+1) for the open shell species (radicals). The resulting CASSCF/STO-3G optimized conformation was used to perform a single point energy and DMA (distibuted multipole analysis) calculation (*31*) with CASSCF in an SV (split valence) 6-31G (*32, 33*) basis set. The active space for these calculations was identical to the active space used in the corresponding CASSCF/STO-3G geometry optimizations.

The use of stabilization energies (heats of reaction, ΔH_R (our ΔE)) for the prediction of metabolite formation in hydrogen atom abstraction reactions catalyzed by P450 is illustrated by Korzekwa *et al.* (*3*). They state that the rates of radical recombination reactions are fast and that the initial hydrogen abstraction is therefore expected to be virtually irreversible. The rate limiting step in the oxidation of the substrate by P450 is therefore assumed to be the hydrogen atom abstraction (*3*). Subsequently, the relative rates of hydroxylation will depend only on the first step, and the relative amounts of products formed will depend primarily on the relative activation energies for hydrogen abstractions at different sites of the molecule. As Korzekwa *et al.* (*3*) found that a linear (Brønsted) relationship exists between stability of radicals (experimental bond dissociation energy data) and activation energies ($\Delta H^{\ddagger}$) of hydrogen abstraction for similar reactions in a series of analogous substrates, the relative order of hydrogen atom abstraction can be obtained simply by calculating the energy difference between a compound and its potential radicals (ΔE). The relatively tedious task of searching for and optimizing transition states can thus be avoided (*3, 34*). On the basis of these observations, the pathways having the most negative ΔE values in our calculations will indicate the most likely sites for hydrogen atom abstraction. The probability at which radical recombination will occur will depend on the distribution of the unpaired electron/spin: sites with a high percentage of the unpaired spin are the most predominant targets for hydroxyl radical recombination, assuming some translational freedom for the formed radical in the active site. So metabolite predictions will depend at least on two phenomena: sites of hydrogen atom abstraction (depending on the stabilization energies) and sites for radical recombination (depending on spin distribution in the radical intermediate).

In the case of enzymatic P450 hydroxylation reactions, the oxygen atom which is inserted into the substrate is supposed to be an activated oxygen bound to the ferric heme iron. In our calculations a single singlet state (in order to comply with conservation of spin) oxygen atom was used as a simplified model for the active site of cytochrome P450 (containing an iron–porphyrin–oxygen moiety). This simplified model reduces the computational efforts required for the calculations significantly. Of the different single oxygen species ^1SO, ^1DO, and ^3PO (with *ab initio* energies of −74.576, −74.696, and −74.777 au, respectively (RHF/SV 6-31G)), ^1SO was used in the calculations. Several years ago, Pudzianowski and Loew indicated a preference for ^3PO as a model for P450 over ^1SO using MINDO/3 calculations (*35*). This assumption however ignores the requirement for conservation of spin. Despite obvious limitations in mimicking P450 oxidations with small molecule gas phase systems, these calculations are useful for several reasons (*3, 34*): (1) The active site of the enzyme is thought to be mainly hydrophobic in nature, which can be approximated by gas phase calculations; (2) most P450 oxidations are thought to involve radical reactions; therefore, charge stabilization by the apoprotein may not be significant during the reaction; (3) the often

Scheme 1. Metabolic Pathways of Anisole (1) Oxidation via the Hydrogen Atom Abstraction, Spin Delocalization, Radical Recombination Mechanism

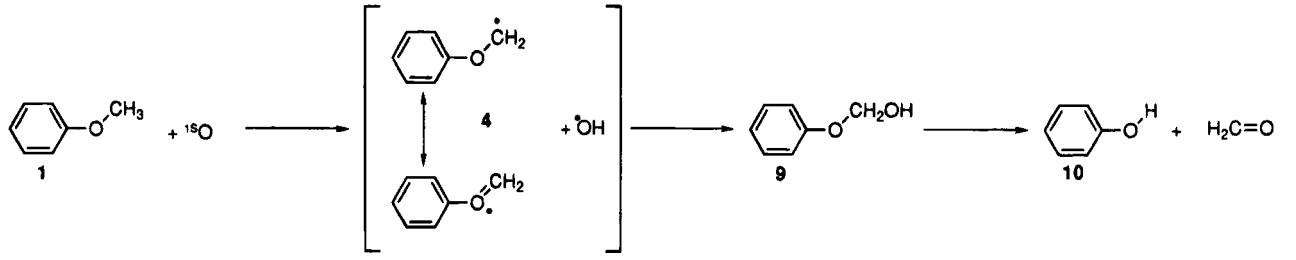

Scheme 2. Metabolic Pathways of *p*-Methylanisole (2) Oxidation via the Hydrogen Atom Abstraction, Spin Delocalization, Radical Recombination Mechanism

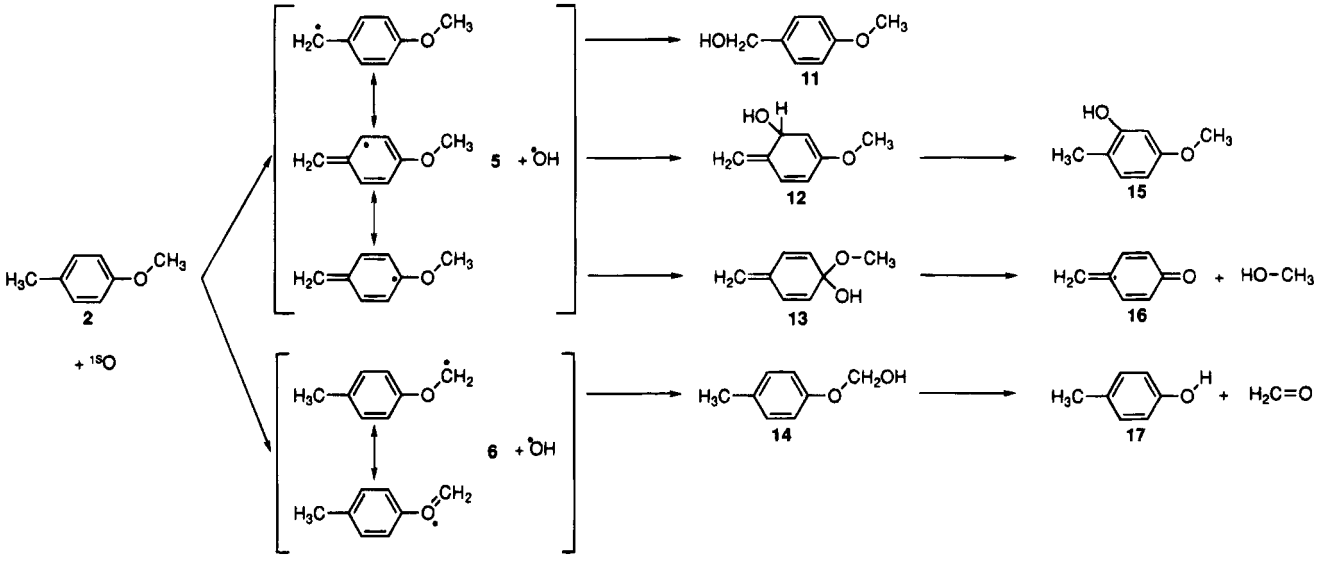

Scheme 3. Metabolic Pathways of *p*-Cyclopropylanisole (3) Oxidation via the Hydrogen Atom Abstraction, Spin Delocalization, Radical Recombination Mechanism

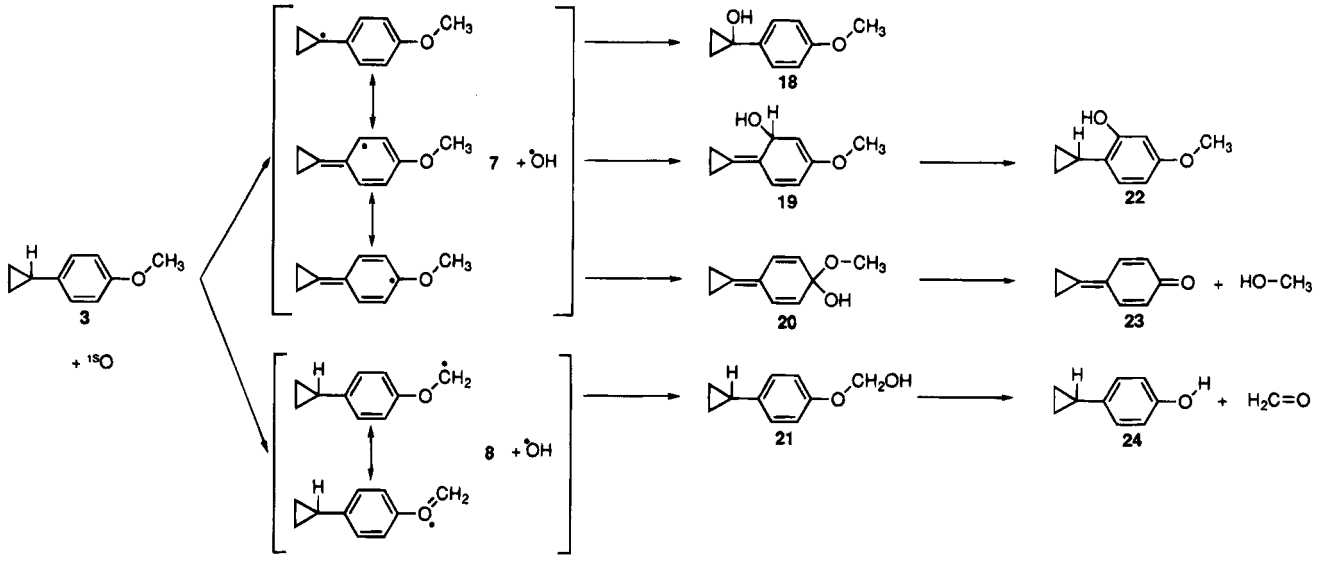

broad regio- and stereoselectivity observed by P450s suggests that oxidation of the substrate mostly is "chemical like" and does not strictly require specific interactions of the substrate with the apoprotein. As no description of the active site can be included in the calculations as yet, no specific conclusions concerning isoenzyme differences can be drawn.

Results and Discussion

The purpose of this study is to rationalize and/or predict the most probable metabolites of hydroxylation by P450 for a series of para-substituted anisoles. The influence of substituents para to the methoxy group at the aromatic ring upon various possible oxidative metabolic routes is investigated. In Schemes 1–3, the oxidative metabolic pathways of anisole (**1**), *p*-methylanisole (**2**), and *p*-cyclopropylanisole (**3**) hypothetically possible via the hydrogen atom abstraction, spin delocalization, hydroxyl radical recombination mechanism are shown. Direct aromatic hydroxylation has not been taken into account. Abstraction of a hydrogen atom from an aro-

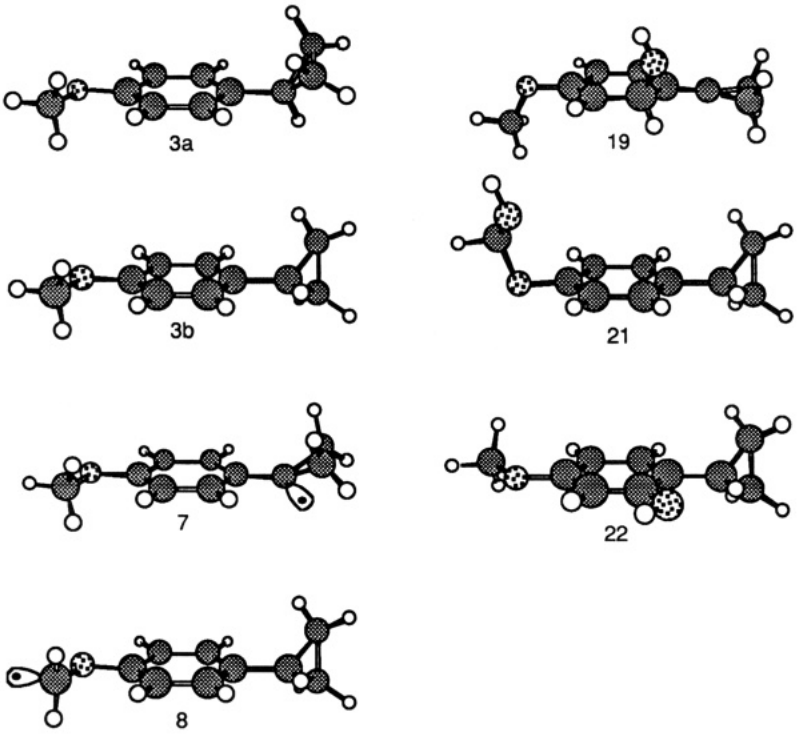

Figure 2. Optimized geometries of *p*-cyclopropylanisole (**3**), radicals **7** and **8**, intermediates **19** and **21**, and metabolite **22** (see also Scheme 3).

matic ring is energetically unfavorable compared to hydrogen atom abstraction from an aliphatic carbon; for example, hydrogen atom abstraction from the methoxy carbon atom of anisole is 50.9 kJ/mol (RHF/SV 6-31G; data not shown) more favorable than hydrogen atom abstraction from the para position of the aromatic ring of anisole (**1**). Furthermore, the hydrogen atom abstraction from the benzylic position of **2** and **3** is respectively 74.5 and 33.0 kJ/mol (RHF/SV 6-31G; data not shown) more favorable than hydrogen atom abstraction from the aromatic ring at the ortho position relative to either the methyl or the cyclopropyl group. The energy differences for primary hydrogen abstraction will, however, not rule out direct aromatic hydroxylation.

Calculated Conformations. The three parent compounds (**1**–**3**) were found to have minimal energy conformations in which the methoxy group is coplanar with the aromatic ring. Cyclopropylarenes exist in either one of two possible conformations, i.e., bisected[2] or perpendicular[2] (*36, 37*). For cyclopropylbenzene the calculated semiempirical energy difference between these two conformations is only 4.6 kJ/mol in favor of the bisected conformation, and the cyclopropyl group is essentially freely rotating (*37*). The estimated experimental value of the energy difference between these conformations is about 5.9 kJ/mol (*38*), with the bisected[2] conformation being the most favorable one. The *ab initio* calculated lowest energy conformation of *p*-cyclopropylanisole (**3**), however, is such that the cyclopropyl group is in a perpendicular[2] conformation (Figure 2: **3a**), while the bisected[2] conformation with the methoxy group positioned *trans* relative to the cyclopropyl moiety (Figure 2: **3b**) is 5.5 kJ/mol higher in energy.

[2] The nomenclature used is derived from Tanko *et al.* (*36*) with bisected ($\Theta = 0°$) and perpendicular ($\Theta = 90°$), where Θ represents the angle defined by the cyclopropyl methine C–H bond with respect to the aromatic plane. As in some radicals the methine hydrogen has been abstracted, the system using the angle Θ has not been used. The designations perpendicular and bisected, however, have been maintained.

The radical formed upon abstraction of a hydrogen atom from the benzylic carbon position of *p*-methylanisole (**2**) (to yield **5**, Scheme 2) appears to have a planar geometry. This calculated geometry is in accordance with the findings of Pacansky *et al.* for a benzylic radical (*39*). Calculations showed that the *p*-methoxyphenyl cyclopropyl radical is in a perpendicular-like[2] conformation (Figure 2: **7**). The geometry of the radicals formed upon abstraction of a hydrogen atom from the *p*-methoxy group of **1**–**3** (i.e., **4**, **6**, and **8**, Schemes 1, 2, and 3, respectively) mimics the geometry of the corresponding parent compound (**1**, **2**, and **3**), e.g., with respect to the cyclopropyl part (compare Figure 2: **3b** and **8**).

The geometries of the aromatic intermediates and products of **3** (**18**, **21**, **22**, and **24**: Scheme 3) are such that the cyclopropyl group is in the bisected[2] conformation (see, e.g., **21** and **22** in Figure 2) with sterically possible interfering substituents pointing in different directions (e.g., **22**, Figure 2). In the case of hydroxylation at the methoxy group (**9**, **14**, and **21**), the methoxy group is rotated out of the aromatic plane (compare Figure 2: **3** and **21**), the dihedral angle ($\tau = C_{methoxy}-O_{methoxy}-C_{ring}-C_{ring}$) being considerably larger in the *p*-cyclopropylanisole intermediate **21** ($\tau = 108.7°$) than in the *p*-methylanisole intermediate **14** ($\tau = 2.0°$). In the case of nonaromatic intermediates in which a double bond connects the para substituent to the ring (**12** and **13**, Scheme 2, **19** and **20**, Scheme 3) the methoxy group is rotated out of the plane of the 6-membered ring (e.g., Figure 2: **19**; $\tau = 75.5°$).

Energy Differences, Radical Spin Distributions, and Product Predictions. Table 1 presents the stabilization energies (ΔE) of the respective hypothetical reactions given in Schemes 1, 2, and 3. Figure 3 shows the unpaired spin distributions of radicals **4**–**8**. Following the lowest energy pathways through Schemes 1–3 and looking at the spin distributions of the radicals, predictions have been made concerning the most likely oxidative metabolites, a procedure which has already

Table 1. Stabilization Energies (CASSCF/SV 6-31G Energies of CASSCF/STO-3G Optimized Geometries)

H-abstraction		recombination		subsequent reaction		
reaction	ΔE (kJ/mol)	reaction	ΔE (kJ/mol)	reaction	ΔE (kJ/mol)	$\Delta E_{overall}$ (kJ/mol)
1 → **4**	−387.5	**4** → **9**	−216.7	**9** → **10**	−96.4	−700.6
2 → **5**	−439.0	**5** → **11**	−178.5			−617.5
		5 → **12**	−67.0	**12** → **15**	−132.5	−638.5
		5 → **13**	−109.4	**13** → **16**	−62.5	−610.9
2 → **6**	−376.4	**6** → **14**	−263.1	**14** → **17**	−50.1	−689.6
3 → **7**	−397.4	**7** → **18**	−225.3			−628.2
		7 → **19**	−70.5	**19** → **22**	−160.5	−633.9
		7 → **20**	−98.7	**20** → **23**	−83.1	−584.7
3 → **8**	−385.9	**8** → **21**	−231.1	**21** → **24**	−80.0	−702.5

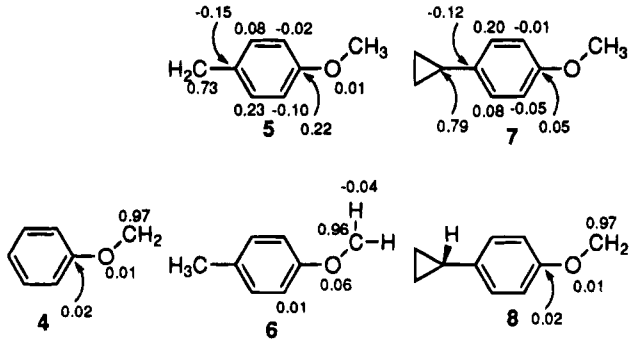

Figure 3. Spin distributions (≥1%) in the intermediate radicals (α-spin). Negative values indicate β-spin.

successfully been used to predict the oxidative metabolites of paracetamol (*7*) and phenacetin (*8*).

Schemes 2 and 3 and the corresponding energy differences in Table 1 reveal that hydrogen atom abstraction from the benzylic C_α-atom of the para substituent is favored over hydrogen atom abstraction from the methoxy group in **2** and **3** (62.6 and 11.5 kJ/mol, respectively; Table 1). For **1** only hydrogen atom abstraction from the methoxy group is possible (Scheme 1) as there is no hydrogen containing para substituent. Following the energetically most favorable pathways for hydrogen atom abstraction leads to abstraction from the methoxy moiety for **1** and hydrogen abstraction from the benzylic C_α-atom for **2** and **3** (Table 1).

The spin distribution of the resulting methoxy radicals (**4**, **5**, and **7**, Schemes 1, 2, and 3, respectively) gives an indication of the relative amounts of metabolites formed. In all radicals (**4**–**8**) the unpaired spin remains mainly localized at the atom from which the hydrogen atom is primarily abstracted (see Figure 3). When a hydrogen atom is abstracted from a methoxy group, localization of unpaired spin is pronounced (**1**: 97%, Figure 3). However, when a benzylic hydrogen atom is abstracted (**2** and **3**), the unpaired spin delocalizes to some extent to the ortho and para carbon nuclei in the aromatic ring (α-spin: 11–16%, Figure 3: positive sign (*40*)) and, apparently, to some extent to the meta and ipso atoms of the aromatic ring as β-spin (see Figure 3: negative sign). The β-spin density at the ipso position, not indicated in Schemes 2 and 3, in principle could after recombination lead to a diradical intermediate. This intermediate would consecutively rearrange to products **11** and **18**, respectively. Therefore, this diradical intermediate has not been subjected to the calculations in this study.

So, radical recombination in case of **1** will mainly take place at the methoxy carbon atom, finally yielding the O-demethylated product **10** and formaldehyde (Scheme 1). On the basis of both the energy differences (Table 1) and the spin distribution data (Figure 3), the radical recombinations for **2** and **3** (Schemes 2 and 3, respectively) will mainly occur at the benzylic carbon atom, yielding products **11** and **18**, respectively, and to some (minor) extent at the ortho and para positions in the aromatic ring, yielding **15** and **16**, and **22** and **23**, respectively. Products **15**, **16** and **22**, **23** are therefore predicted to be minor oxidative metabolites of **2** and **3**, respectively. As **16** and **23** are alkylating agents like *N*-acetyl-*p*-benzoquinone imine (NAPQI) (*41*, *42*), they may lead to inactivation of P450. Intermediates **13** and **20** resemble the hypothetical intermediates formed during the activation of phenacetin (*8*).

The O-demethylated product **24** (Scheme 3) was recently detected experimentally (*20*). The formation of the O-demethylated products **17** and **24** and formaldehyde (Schemes 2 and 3), via the energetically relatively unfavorable radicals **6** and **8** (**2** → **6** and **3** → **8**, Table 1), and the respective carbinol intermediates (**14** and **21**), is also predicted to be of minor importance. The formation of product **24** and formaldehyde via radical **8** might however be expected to be somewhat more abundant than the formation of product **17** and formaldehyde via radical **6**, as the stabilization energies of radicals **7** and **8** are more alike (−397.4 and −385.9 kJ/mol, respectively; Table 1) than the stabilization energies of radicals **5** and **6** (−439.0 and −376.4 kJ/mol, respectively; Table 1).

When comparing the stabilization energies (ΔE) of the formation of radicals **4**, **6**, and **8** (Table 1), variation of the para substituent appears to result in small energy differences for hydrogen atom abstraction from the methoxy group, as well as in similar (albeit small) spin distribution in these radicals (**4**, **6**, and **8**: Figure 3). Comparison of radicals **5** and **7** indicates larger differences in spin distribution (Figure 3). Formation of benzylic radical **5** is 41.6 kJ/mol more favorable than formation of cyclopropyl radical **7** (Table 1). Spin delocalization is more pronounced in radicals **5** and **7** than in radicals **4**, **6**, and **8** (Figure 3).

Comparison with Experimental Data. In case of anisole (**1**) (as direct aromatic hydroxylation is not considered in this study), we predict only radical **4** to be formed, which is subsequently proposed to lead to formation of product **10** and formaldehyde (Scheme 1). Anodic acetoxylation of anisole (**1**) is reported to produce mainly ortho- and para-acetylated products (*14*). This is, however, not a radical reaction and therefore cannot be seen as experimental support for the present predictions. The chemical oxidation of *p*-methylanisole (**2**) with manganese(III) acetate, and a variety of other one-electron chemical oxidants, has been shown to result in acetylation of the benzylic carbon (*14*, *15*), finally primarily yielding *p*-methoxybenzyl alcohol (**11**) (*16*). Our predictions are in agreement with this result (Table 1, Scheme 2). A different mechanism might be responsible for these chemical oxidations, although not necessarily (*16*).

Recently, Riley and Hanzlik (*20*) investigated the metabolism of *p*-cyclopropylanisole (**3**) in differentially induced rat liver microsomes. The main metabolites were found to be **18** and **24** (*20*). The formation of **18** is in good agreement with our predictions (Scheme 3). Also, the formation of **24** in appreciable amounts can be explained when taking into account the relatively small energy difference between the stabilization of radicals **7** and **8**, and the parent compound **3** (Table 1, Scheme 3). Experimentally, however, the amount of **24** formed (90% of the metabolites found) exceeded the amount of **18** formed significantly (*20*). The same authors did not find cyclopropyl ring opened metabolites, which is also consistent with the proposed hydrogen atom abstraction and radical recombination mechanism. The observed P450 inactivation was explained with hypothetical cyclopropyl ring opened structures covalently binding to the protein (*20*). In our concept, however, this phenomenon could result from the minor metabolite **23**, which may alkylate P450s like, e.g., NAPQI (*41, 42*). The minor 4-cyclopropylidene-2,5-cyclohexadien-1-one metabolite **23** was not detected experimentally, while metabolite **22** was only detected in βNF (β-naphthoflavone)-induced rat liver microsomes (*20*).

Except for the metabolism of **3**, Riley and Hanzlik also studied the metabolism of cyclopropylbenzene in rat liver microsomes. The experimentally observed metabolites were 1-phenylcyclopropanol, 4-cyclopropylphenol, and 2-cyclopropylphenol. A general mechanistic scheme was presented in which the formation of 1-phenylcyclopropanol was explained via a hydrogen abstraction, radical recombination reaction. However, the remaining metabolites were assumed to be formed via different mechanisms involving direct reactions with the aromatic ring (e.g., one-electron abstraction from the aromatic ring and subsequent proton abstraction, direct addition of a ferryl oxygen to a π-bond or lone pair), while inactivation was assumed to occur via ring opened metabolites which were not detected (*20*). In our concept, the formation of all observed metabolites as well as the enzyme inactivation could be explained solely by using the formalism of hydrogen atom abstraction, spin delocalization, and radical recombination. The experimental observation was that only in βNF-induced rat liver microsomes was the formation of 2-cyclopropylphenol (a metabolite we would predict to be formed to a minor extent) detected, in contrast to phenobarbital-induced rat liver microsomes. Calculations like ours, however, cannot explain differences between isoenzymes until sterical requirements of the active sites of the various isoenzymes are considered. Besides the sterical influence of the enzyme on the orientation of the substrate, the active site of isoenzyme also might electronically influence the spin distribution of the formed radicals. However, as yet no accurate geometry of microsomal P450 active sites is available.

Conclusions

Anisole (**1**) is predicted to be metabolized, via a hydrogen atom abstraction, spin delocalization, radical recombination mechanism, at the methoxy carbon atom. In case a *p*-methyl or *p*-cyclopropyl substituent is added to obtain compounds **2** and **3**, metabolism is predicted to occur via initial abstraction of a hydrogen atom from the benzylic carbon, forming the intermediate radicals **5** and **7** and finally yielding hydroxylated products **11** and **18**. Hydrogen atom abstraction from the methoxy group, via radicals **6** and **8** and intermediates **14** and **21** leading to the oxygen-demethylated products **17** and **24** and formaldehyde, is less favorable. Comparison of the mayor metabolites of *p*-cyclopropylanisole (**3**) predicted to be formed with recent experimental microsomal metabolism data indicates that both metabolites, indicated to be most likely according to our calculations, **18** and **24**, are indeed formed.

Combining calculated energy difference and spin delocalization data (on parent compounds, metabolic intermediates, and products) allowed a correct rationalization of most favored products, although a quantitative measure for the relative amounts is still hard to obtain. Hydrogen atom abstraction energies for hydrogen atom abstraction from a methoxy group are hardly influenced by para substitution of the aromatic ring with a methyl or a cyclopropyl substituent. Hydrogen atom abstraction from the benzylic carbon atom of the para substituent is primarily determined by the stability of the radical formed. When a hydrogen atom can be abstracted from the para substituent giving a benzylic radical, this pathway is favored over hydrogen atom abstractions from other positions (like a methoxy group) according to our calculations.

Acknowledgment. IBM is gratefully acknowledged for providing RISC RS6000 workstations and NCF (Nederlandse Computer Faciliteiten) for supercomputer facilities. Use of the Silicon Graphics Challenge of the Faculty of Chemistry of the Utrecht University is gratefully acknowledged. We express our gratitude to Prof. Dr. Robert P. Hanzlik and Dr. Pamela Riley for providing experimental data concerning the metabolism of some of the compounds presented in this study prior to publication.

References

(1) Guengerich, F. P., and MacDonald, T. L. (1990) Mechanisms of cytochrome P-450 catalysis. *FASEB J.* **4**, 2453–2459.

(2) White, R. E. (1991) The involvement of free radicals in the mechanism of monooxygenases. *Pharmacol. Ther.* **49**, 21–42.

(3) Korzekwa, K. R., Jones, J. P., and Gilette, J. R. (1990) Theoretical studies on cytochrome P-450 mediated hydroxylation: A predictive model for hydrogen atom abstractions. *J. Am. Chem. Soc.* **112**, 7042–7046.

(4) Guengerich, F. P., and MacDonald, T. L. (1984) Chemical mechanisms of catalysis by cytochromes P-450: A unified view. *Acc. Chem. Res.* **17**, 9–16.

(5) Ortiz de Montellano, P. R., and Stearns, R. A. (1989) Radical intermediates in the cytochrome P-450-catalysed oxidation of aliphatic hydrocarbons. *Drug Metab. Rev.* **20**, 183–191.

(6) Ortiz de Montellano, P. R. (1989) Cytochrome P-450 catalysis: radical intermediates and dehydrogenation reactions. *Trends Pharmcol. Sci.* **10**, 354–359.

(7) Koymans, L. M. H., Lenthe, J. H. v., Straat, R. v. d., Donné-Op den Kelder, G. M., and Vermeulen, N. P. E. (1989) A theoretical study on the metabolic activation of paracetamol by cytochrome P-450: indications for a uniform oxidation mechanism. *Chem. Res. Toxicol.* **2**, 60–66.

(8) Koymans, L. M. H., Lenthe, J. H. v., Donné-Op den Kelder, G. M., and Vermeulen, N. P. E. (1990) Mechanisms of activation of phenacetin to reactive metabolites by cytochrome P-450: a theoretical study involving radical intermediates. *Mol. Pharmacol.* **37**, 452–460.

(9) Ohe, T., Mashino, T., and Hirobe, M. (1994) Novel metabolic pathway of arylethers by cytochrome P450: cleavage of the oxygen-aromatic ring bond accompanying *ipso*-substitution by the oxygen atom of the active species in cytochrome P450 models and cytochrome P450. *Arch. Biochem. Biophys.* **310**, 402–409.

(10) Hanzlik, R. P., and Tullman, R. H. (1982) Suicidal inactivation of cytochrome P-450 by cyclopropylamines. Evidence for cation-radical intermediates. *J. Am. Chem. Soc.* **104**, 2048–2050.

(11) Ortiz de Montellano, P. R. (1986) *Cytochrome P-450: structure, mechanism, and biochemistry,* p 556, Plenum Press, New York.
(12) Cnubben, N. H. P., Vervoort, J., Veeger, C., and Rietjens, I. M. C. M. (1992) Study of the regioselectivity and mechanism of the aromatic hydroxylation of monofluoroanilines. *Chem.-Biol. Interact.* **85**, 151–172.
(13) Stearns, R. A., and Ortiz de Montellano, P. R. (1985) Cytochrome P-450 catalysed oxidation of quadricyclane. Evidence for a radical cation intermediate. *J. Am. Chem. Soc.* **107**, 4081–4082.
(14) Eberson, L. (1967) Studies on electrolytic substitution reactions. III. Isomer distributions and isotope effects in nuclear and side-chain anodic acetoxylation of aromatic compounds. *J. Am. Chem. Soc.* **89**, 4669–4677.
(15) Andrulis, P. J., Dewar, M. J. S., Dietz, R., and Hunt, R. L. (1966) Aromatic oxidation by electron transfer. I. Oxidations of p-methoxytoluene. *J. Am. Chem. Soc.* **88**, 5473–5478.
(16) Riley, P., and Hanzlik, R. P. (1989) Free radical chlorination and one-electron oxydation of arylcyclopropanes. Designer probes for cytochrome P-450 hydroxylation mechanisms. *Tetrahedron Lett.* **30**, 3015–3018.
(17) Shono, T., and Matsumara, Y. (1970) Organic synthesis by electrolysis. VI. Anodic oxydation of arylcyclopropanes. *J. Org. Chem.* **35**, 4157–4160.
(18) Hanzlik, R. P., and Ling, K. H. J. (1990) Active site dynamics of toluene hydroxylation by cytochrome P-450. *J. Org. Chem.* **55**, 3992–3997.
(19) Ling, K. H. J., and Hanzlik, R. P. (1989) Deuterium isotope effects on toluene metabolism. Product release as a rate-limiting step in cytochrome P-450 catalysis. *Biochem. Biophys. Res. Commun.* **160**, 844–849.
(20) Riley, P., and Hanzlik, R. P. (1994) Electron transfer in P450 mechanisms. Microsomal metabolism of cyclopropylbenzene and p-cyclopropylanisole. *Xenobiotica* **24**, 1–16.
(21) Korzekwa, K., Trager, W., Gouterman, M., Sprangler, D., and Loew, G. H. (1985) Cytochrome P450 mediated aromatic oxydation: a theoretical study. *J. Am. Chem. Soc.* **107**, 4273–4279.
(22) Dupuis, M., Spangler, D., and Wendoloski, J. (1980) NRCC Program No. QG01 (GAMESS).
(23) Guest, M. F., Lenthe, J. H. v., Kendrick, J., Schoffel, K., Sherwood, P., Harrison, R. J., with contributions from: Amos, R. D., Buenker, R. J., Dupuis, M., Handy, N. C., Hillier, I. H., Knowles, P. J., Bonacic-Koutecky, V., Niessen, W. v., Saunders, V. R., and Stone, A. J. (1993) GAMESS-UK, IBM RS6000 v2.1.
(24) Chemical Design Ltd., ChemX, version January 1990.
(25) Hehre, W. J., Stewart, R. F., and Pople, J. A. (1969) Self consistent molecular orbital methods. I. Use of Gaussian expansions of Slater-type atomic orbitals. *J. Chem. Phys.* **51**, 2657–2664.
(26) Roos, B. O., Linse, P., Siegbahn, P. E. M., and Blomberg, M. R. A. (1982) A simple method for the evaluation of the second-order perturbation energy from external double-excitations with a CASSCF reference wavefunction. *Chem. Phys.* **66**, 197–207.
(27) Knowles, P. J., Sexton, G. J., and Handy, N. C. (1982) Studies using the CASSCF wavefunction. *Chem. Phys.* **72**, 337–347.
(28) Knowles, P. J., and Werner, H. J. (1985) An efficient second-order MC SCF method for long configuration expansions. *Chem. Phys. Lett.* **115**, 259–269.
(29) Pulay, P., and Hamilton, T. P. (1988) UHF natural orbitals for defining and starting MC-SCF calculations. *J. Chem. Phys.* **88**, 4926–4933.
(30) Bofill, J. M., and Pulay, P. (1989) The unrestricted natural orbital-complete active space (UNO-CAS) method: An inexpensive alternative to the complete active space-self-consistent-field (CAS-SCF) method. *J. Chem. Phys.* **90**, 3637–3646.
(31) Stone, A. J. (1981) Distributed multipole analysis, or how to describe a molecular charge distribution. *Chem. Phys. Lett.* **83**, 233–239.
(32) Binkley, J. S., Pople, J. A., and Hehre, W. J. (1980) Self consistent molecular orbital methods. 21. Small split-valence basis sets for first-row elements. *J. Am. Chem. Soc.* **102**, 939–947.
(33) Gordon, M. S., Binkley, J. S., Pople, J. A., Pietro, W. J., and Hehre, W. J. (1982) Self consistent molecular orbital methods. 22. Small split-valence basis sets for second-row elements. *J. Am. Chem. Soc.* **104**, 2797–2803.
(34) Korzekwa, K. R., and Jones, J. P. (1993) Predicting the cytochrome P450 mediated metabolism of xenobiotics. *Pharmacogenetics* **3**, 1–18.
(35) Pudzianowski, A., and Loew, G. H. (1980) Quantum-chemical studies of model cytochrome P450 hydrocarbon oxidation mechanisms. 1. A MINDO/3 study of hydroxylation and epoxidation pathways for methane and ethylene. *J. Am. Chem. Soc.* **102**, 5443–5449.
(36) Tanko, J. M., Mas, R. H., and Suleman, N. K. (1990) Stereoelectronic effects on chemoselectivity in the free radical bromination of arylcyclopropanes. *J. Am. Chem. Soc.* **112**, 5557–5562.
(37) Drumright, R. E., Mas, R. H., Merola, J. S., and Tanko, J. M. (1990) Interplay between conjugative and steric effects in cyclopropylarenes. *J. Org. Chem.* **55**, 4098–4102.
(38) Closs, G. L., and Klinger, H. B. (1965) Determination of conformational preference in arylcyclopropanes by nuclear magnetic resonance. *J. Am. Chem. Soc.* **87**, 3265–3266.
(39) Pacansky, J., Liu, B., and DeFrees, D. (1986) Theoretical structures for the phenyl and benzyl radicals. *J. Org. Chem.* **51**, 3720–3721.
(40) McMurry, J. (1984) Arenes: synthesis and reactions of alkylbenzenes. In *Organic Chemistry* (Needham, M., Ed.) pp 534–535, Brooks/Cole Publishing Co., Monterey.
(41) Hinson, J. A., Nelson, S. D., and Mitchell, J. R. (1977) Studies on the microsomal formation of arylating metabolites of acetaminophen and phenacetin. *Mol. Pharmacol.* **13**, 625–633.
(42) Nelson, S. D., Forte, A. J., Vaishnav, Y., Mitchell, J. R., Gillette, J. R., and Hinson, J. A. (1981) The formation of arylating and alkylating metabolites of phenacetin in hamsters and hamster liver microsomes. *Mol. Pharmacol.* **19**, 140–145.

TX940124N